

Ballistic electron transport exceeding 160 μm in an undoped GaAs/AlGaAs FET

G. R. Facer[†], B. E. Kane, A. S. Dzurak, R. J. Heron, N. E. Lumpkin and R. G. Clark
*Semiconductor Nanofabrication Facility,
University of New South Wales, Sydney NSW 2052 AUSTRALIA*

L. N. Pfeiffer and K. W. West
*Bell Laboratories, Lucent Technologies, Murray Hill NJ 07974 USA
(May 2, 2017)*

We report measurements of GaAs/AlGaAs undoped field-effect transistors in which two-dimensional electron gases (2DEGs) of exceptional quality and versatility are induced without modulation doping. Electron mobilities at $T = 4.2$ K and density $3 \times 10^{11} \text{ cm}^{-2}$ exceed $4 \times 10^6 \text{ cm}^2\text{V}^{-1}\text{s}^{-1}$. At lower temperatures, there is an unusually large drop in scattering, such that the mobility becomes too high to measure in $100 \mu\text{m}$ samples. Below $T = 2.5$ K, clear signatures of ballistic travel over path lengths in excess of $160 \mu\text{m}$ are observed in magnetic focusing experiments. Multiple reflections at the edges of the 2DEG indicate a high degree of specularity.

72.15.Lh,73.23.Ad,73.50.Gr

High quality two-dimensional electron systems in GaAs/Al_xGa_{1-x}As heterostructures form the basis for most semiconductor mesoscopic devices, because they have for some time been used successfully to achieve long mean free paths in the electron layer. To date, modulation-doped (MD) structures, where dopants spatially separated from the GaAs/AlGaAs junction induce a two-dimensional electron gas (2DEG), have yielded the highest electron mobilities^{1,2}.

In 2DEGs where the mean free path becomes comparable to the device dimensions, oscillations in four-terminal resistance measurements can be seen in small magnetic fields B . The B -periodic component corresponds to the electron cyclotron orbit diameter passing through integer divisors of the sample size. This classical phenomenon, referred to as electron focusing^{3,4}, relies on scattering-free or *ballistic* transport across the device. Extensive work has been performed on electron focusing in 2DEGs over a wide range of device sizes ($< 1 \mu\text{m}$ to $150 \mu\text{m}$)^{5,6}. In addition to the many experiments which have been performed to investigate striking behaviour such as fractal self-similarity in the magnetoresistance of very small samples⁷, and the development of ballistic electron optics^{8,9}, electron mobility improvement through further development of epitaxial growth techniques has resulted in the observation of focusing effects up to length scales of order $150 \mu\text{m}$ ⁶.

Saku *et al* have predicted¹⁰ that the highest obtainable mobility in MD systems with electron densities $N \sim 3 \times 10^{11} \text{ cm}^{-2}$ is likely to be $\approx 1.6 \times 10^7 \text{ cm}^2\text{V}^{-1}\text{s}^{-1}$.

This prediction is based on scattering from the potential landscape contributed by randomly located ionized dopants themselves. However, recent experimental studies on MD structures^{1,2} have presented strong evidence that the effect of dopant disorder is not as severe as expected from that model. Whether or not the inherent dopant disorder is the limiting factor for the mobility, there is a way to avoid its effects: the 2DEG can be induced by a gate bias in an accumulation-mode undoped field-effect transistor (UFET)^{11,12}. As the name implies, UFETs contain a high quality, variable-density 2DEG without the use of modulation doping. We report magnetoresistance measurements in several UFETs, where a series of sharp magnetic focusing peaks demonstrate ballistic transport across $100 \mu\text{m}$ devices over the wide density range $N = 2 \times 10^{11} \text{ cm}^{-2}$ to $6 \times 10^{11} \text{ cm}^{-2}$, with ballistic scattering lengths exceeding $160 \mu\text{m}$ established in small magnetic fields at high densities.

The 2DEGs under investigation form at a GaAs/AlGaAs heterojunction upon applying a positive bias to an epitaxially-grown top gate¹¹ (Fig. 1(a)). The lack of dopant-induced disorder greatly reduces scattering, in particular the small-angle scattering from distant ions¹³. UFETs also allow precise tuning of the electron sheet density over nearly two orders of magnitude.

Optical lithography was used to fabricate UFETs configured as squares with side length $100 \mu\text{m}$ (Fig. 1(b, c)). The 2DEG is measured via self-aligned ohmic contacts¹¹. Van der Pauw resistance measurements have been performed in a dilution refrigerator using low-frequency (~ 15 Hz) lock-in techniques with currents less than 150 nA . The temperature-dependent data were taken with gate leakage less than 300 pA . Practical device sizes in the wafers reported here are limited to $\sim 100 \mu\text{m}$ by the presence of oval defects which can cause a short circuit between the gate and the 2DEG.

Electron density and mobility at $T = 4.2$ K are shown in Fig. 2 as a function of top gate voltage. The electron mobility peaks at a density $N \approx 3 \times 10^{11} \text{ cm}^{-2}$, an effect which is more pronounced at temperatures below $T = 1$ K. The presence of this mobility peak is believed to be due to the increasing influence of interface roughness at higher gate voltages, as the 2DEG is pulled closer to the GaAs/AlGaAs heterojunction. The scattering lengths given for the 4.2 K data in Fig. 2 are simply determined from the mobility. The highest values are of order half

the sample size.

Below $T = 4.2$ K, the electron mobility is expected to improve due to the reduction of electron-phonon scattering. If the mean free path exceeds the device dimensions, then a meaningful sheet resistivity cannot be defined, and thus a conventional electron mobility cannot be determined. Instead, the scattering length of the electrons must be used to describe the quality of the 2DEG system.

In the UFET samples, for $T < 4.2$ K, magnetoresistance oscillations are visible at fields on the order of 0.01 T, shown in Fig. 3(a). The vertical axis is the four-terminal measurement¹⁴ $R_{12,43} = (V_4 - V_3)/I_{1\rightarrow 2}$. Near $B = 0$, the measurement can actually be negative, as seen in Fig. 3(a), because electrons are injected directly along the diagonal of the device into the negative voltage-measuring contact V_3 ^{6,14}. Focusing-related oscillations are expected to be periodic in B at any given density, and the field position B_{foc} of the first peak scales as the square root of N :

$$B_{foc} = \frac{2\hbar\sqrt{2\pi N}}{eL}, \quad (1)$$

where L is the size of the device. The experimentally observed oscillations are B -periodic, and the wide tunability of the UFET electron density allows analysis of the density dependence. Fig. 3(b) gives the oscillation positions (maxima) as a function of electron density. The solid curves in the figure show that the periods are consistent with an increase as the square root of N . Note the large magnitude of the oscillations relative to the background signal; no subtraction of a background level is necessary for this data. The number of visible oscillations is related to the specularly of reflections at the edges of the UFET, rather than to the scattering lengths within the 2DEG region. Specularity becomes relevant because each successive peak corresponds to an added skipping orbit. Observation of several consecutive oscillations (labeled a , b , c , d in Fig. 3) indicates that the reflections from the UFET boundaries are highly specular.

Oscillations at a range of temperatures, normalized to the base temperature limit, are shown in Fig. 3(c). Notably, there is a significant temperature dependence below $T = 1$ K, which is stronger than the mobility change, dominated by electron-phonon scattering, usually observed in MD structures¹⁵⁻¹⁷.

Magnetoresistance data spanning both field polarities (B^+ and B^-) are shown in Fig. 4(a). For a diameter of $100 \mu\text{m}$, Eq. (1) predicts a position of the first peak $B_{foc} = 1.98$ mT. The vertical, dotted lines in Fig. 4(a) mark $B = \pm 1.98$ mT, and it can be seen that the experimental data agree very well with the predicted B_{foc} . The electron focusing peaks therefore imply that the ballistic mean free path is at least $(\pi/2 \times 100) \approx 160 \mu\text{m}$. Indeed, given the strength of the oscillations (recalling that there is no background subtraction), the path length probably exceeds this value, but explicit confirmation requires larger samples which are constrained by the oval defects in these high-mobility wafers, described earlier.

At the lowest temperatures, there is an antisymmetric background slope near $B = 0$, which is visible only for $|B| \lesssim 100$ mT. This slope is believed to be related to the Hall effect, and is evident even in the standard four-terminal geometry because of the ballistic nature of transport in the UFETs.

Although the observed position of the first B^+ and B^- focusing peaks agrees well with the predicted B_{foc} , the subsequent period ΔB separating successive oscillations is larger than B_{foc} by 20 %. A larger ΔB indicates a tighter (i.e. *smaller*-diameter) cyclotron orbit than is expected for the $100 \mu\text{m}$ devices. While there are several possible reasons why ΔB could be greater than B_{foc} , such as the lack of four-fold symmetry in the device or anisotropy of injection/absorption of electrons at the self-aligned ohmic contacts (which have resistances ~ 2 k Ω), a convincing explanation of why $\Delta B > B_{foc}$ is yet to be found.

Fig. 4(b) shows data from UFETs made from two wafers. The trace at higher resistance (labeled “Wafer B”) is data taken as part of a far-infrared photoconductivity study¹⁸ which has yielded a very narrow cyclotron resonance linewidth (full width at half maximum) of 6 mT at $T = 1.6$ K and at a wavelength of $183.4 \mu\text{m}$. The wafer B sample has the lower $T = 4.2$ K mobility of $1 \times 10^6 \text{ cm}^2\text{V}^{-1}\text{s}^{-1}$, for $N = 3.6 \times 10^{11} \text{ cm}^{-2}$. The ballistic transport oscillations in the “Wafer A” trace are much better resolved. The different form of the traces from 2DEGs of unequal quality also highlights another aspect of the ballistic transport data: the $B = 0$ resistance minimum, used in itself in previous studies⁶ as evidence for ballistic transport for which sequential peaks are barely resolved, is far more robust than the later focusing peaks, which degrade to a broader envelope.

Several length scales have been used to describe scattering in high-mobility semiconductor heterostructures. To minimize confusion, we employ the convention of Spector *et al.*^{5,8}. The most commonly used distance is the elastic mean free path λ_μ , which is the distance derived from mobility calculations. λ_μ is the distance over which an electron travels before its momentum is completely randomized. Next, there is a ballistic mean free path λ_b which is the distance over which ballistic focusing peaks are visible. λ_b is more sensitive to small-angle scattering than λ_μ , since several small-angle scattering events are required to fully randomize the motion of an electron, whereas ballistic focusing relies fundamentally on directional effects. In the case of these UFETs, there will be a small angular tolerance introduced by the finite width of the corner constrictions (Fig. 1(b)). Finally, there is λ_q , the length which is obtained via the quantum lifetime from Shubnikov-de-Haas oscillations¹⁹. λ_q is expected to be the smallest of all the various path lengths¹⁹; in GaAs/AlGaAs systems, generally $\lambda_\mu > \lambda_b > \lambda_q$.

Related to λ_q is the lifetime obtained via cyclotron resonance measurements. The 6 mT resonance linewidth stated above for wafer B yields a scattering lifetime of 130 ps in a low density regime ($N = 2.7 \times 10^{10} \text{ cm}^{-2}$). If

one naïvely multiplies this lifetime by the Fermi velocity, a path length of $9\ \mu\text{m}$ is obtained, attesting to the high quality of even the lower-mobility wafer B sample.

It is known that the ionized dopants in modulation-doped structures act as small-angle scatterers¹⁹, in addition to scattering by any random intrinsic impurities. In a recent study of modulation-doped layers, Umansky *et al.*¹ report a mobility at $T = 0.1\ \text{K}$ of $1.44 \times 10^7\ \text{cm}^2\text{V}^{-1}\text{s}^{-1}$. In that paper, the authors calculate that the dopants contribute only 10 percent of the total scattering. The mobility yields $\lambda_\mu \gtrsim 110\ \mu\text{m}$ at the stated $N = 2.4 \times 10^{11}\ \text{cm}^{-2}$, which we note is smaller than the λ_b of $160\ \mu\text{m}$ in wafer A above. A previous study of λ_b in MD structures with $\mu = 1.1 \times 10^7\ \text{cm}^2\text{V}^{-1}\text{s}^{-1}$ also indicated that the dominant scattering at $T < 0.5\ \text{K}$ is large-angle, probably due to impurities at the heterojunction interface⁸. In the same paper, the ratio of the elastic and ballistic mean free paths was found to be $\lambda_\mu/\lambda_b \approx 6$. Applying the same factor to the ballistic mean free path data reported here would imply a mobility greater than $10^8\ \text{cm}^2\text{V}^{-1}\text{s}^{-1}$ and $\lambda_\mu \sim 1\ \text{mm}$; therefore it is likely that the ratio λ_μ/λ_b in the UFET samples is less than that in MD structures.

A mechanism which may be relevant to the T -dependence of the focusing peak amplitudes is electron-electron interaction. Electron-electron scattering is expected to depend on T as $T^2 \log(T/T_F)$, where T_F is the Fermi temperature²⁰. While it is not expected that electron-electron interactions should have a significant effect on the resistivity, such interactions have been demonstrated to have an impact on resistance measurements of smaller devices in a ballistic transport regime²¹. The amplitude data in the inset to Fig. 3(c) do not fit such a temperature dependence well, although a one-to-one correspondence between the interaction rate and the peak amplitudes should not necessarily be expected. The precise mechanism involved in the large mean free path improvement below $T = 4.2\ \text{K}$ is therefore yet to be identified.

Even if mobilities in MD structures improve substantially, UFET samples will prove of greatest benefit in the production of one- or zero-dimensional structures. This is because, in nanostructures, even the minimal fluctuations caused by dopants (sufficient only to cause small-angle scattering in a 2DEG) are enough to significantly perturb the potential landscape, and thus the device behaviour²². In addition, mean free paths improve as N increases, enhancing the worth of the tunability of UFETs to very high N : in MD structures, high densities are attainable only by bringing the dopants closer to the 2DEG, with a corresponding increase in disorder. We have recently reported²³ ballistic transport in quantum wires fabricated from the UFET material described in Fig. 1.

In summary, ballistic path lengths of $160\ \mu\text{m}$, limited by practical UFET device sizes, have been demonstrated in GaAs/AlGaAs UFETs free from dopant disorder. Such long ballistic paths show that non-modulation-

doped FETs can contain 2DEGs of exceptionally high quality. The fact that ballistic mean free paths exceed the dimensions of the device mean that conventional diffusive descriptions of the electron behaviour, in terms of mobility and resistivity, are no longer appropriate. A substantial improvement in scattering length as a function of temperature below $T = 4.2\ \text{K}$, greater than has been reported in recent high-mobility modulation-doped 2DEGs, has also been observed.

This work was supported by the Australian Research Council.

[†] E-mail: gfacer@newt.phys.unsw.edu.au

- ¹ V. Umansky, R. de Picciotto, and M. Heiblum, *Appl. Phys. Lett.* **71**, 683 (1997).
- ² L. N. Pfeiffer, private communication, (1998).
- ³ H. van Houten *et al.*, *Phys. Rev. B* **39**, 8556 (1989).
- ⁴ C. T. Foxon *et al.*, *Semicond. Sci. and Technol.* **4**, 582 (1989).
- ⁵ J. Spector *et al.*, *Surf. Sci.* **228**, 283 (1990).
- ⁶ Y. Hirayama, T. Saku, S. Tarucha, and Y. Horikoshi, *Appl. Phys. Lett.* **58**, 2672 (1991).
- ⁷ R. P. Taylor *et al.*, *Phys. Rev. B* **51**, 9801 (1995).
- ⁸ J. Spector *et al.*, *Surf. Sci.* **263**, 240 (1990).
- ⁹ J. Spector *et al.*, *Appl. Phys. Lett.* **56**, 967 (1990).
- ¹⁰ T. Saku, Y. Horikoshi, and Y. Tokura, *Jpn. J. Appl. Phys.* **1** **35**, 34 (1996).
- ¹¹ B. E. Kane, L. N. Pfeiffer, and K. W. West, *Appl. Phys. Lett.* **67**, 1262 (1995).
- ¹² J. Herfort and Y. Hirayama, *Solid-State Electronics* **41**, 1535 (1997).
- ¹³ S. Das Sarma and F. Stern, *Phys. Rev. B* **32**, 8442 (1985).
- ¹⁴ M. Büttiker, *Phys. Rev. Lett.* **57**, 1761 (1986).
- ¹⁵ H. L. Stormer, L. N. Pfeiffer, K. W. Baldwin, and K. W. West, *Phys. Rev. B* **41**, R1278 (1990).
- ¹⁶ E. E. Mendez, P. J. Price, and M. Heiblum, *Appl. Phys. Lett.* **45**, 294 (1984).
- ¹⁷ L. N. Pfeiffer, K. W. West, H. L. Stormer, and K. W. Baldwin, *Appl. Phys. Lett.* **55**, 1888 (1989).
- ¹⁸ R. J. Heron *et al.*, *Bulletin of the APS* **43**, 43 (1998).
- ¹⁹ T. Ando, M. Fowler, and F. Stern, *Rev. Mod. Phys.* **54**, 437 (1982).
- ²⁰ G. F. Giuliani and J. J. Quinn, *Phys. Rev. B* **26**, 4421 (1982).
- ²¹ L. W. Molenkamp and M. J. M. de Jong, *Phys. Rev. B* **49**, 5038 (1994).
- ²² J. A. Nixon, J. H. Davies, and H. U. Barranger, *Phys. Rev. B* **43**, 12638 (1991).
- ²³ B. E. Kane *et al.*, *Appl. Phys. Lett.* (accepted for publication, 1998).

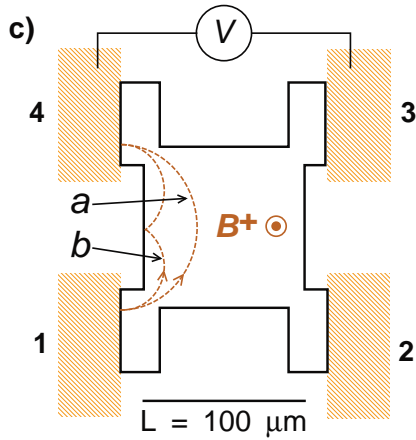
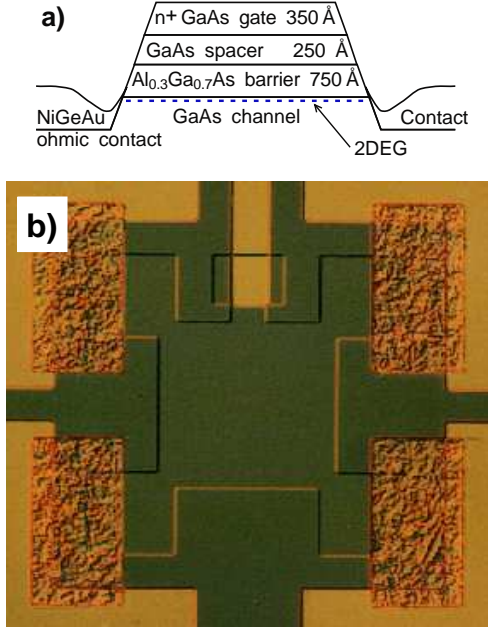


FIG. 1. (a) Layer structure of the FET devices. (b) Optical microscope picture of a UFET device: the width of the central square is $100 \mu\text{m}$. Mottled regions in the corners are self-aligned ohmic contacts which make contact to the electron layer without a short circuit to the top gate. (c) Schematic diagram, defining the labelling convention for the current $I_{1 \rightarrow 2}$, and the measured voltage $V_4 - V_3$, between ohmic contacts.

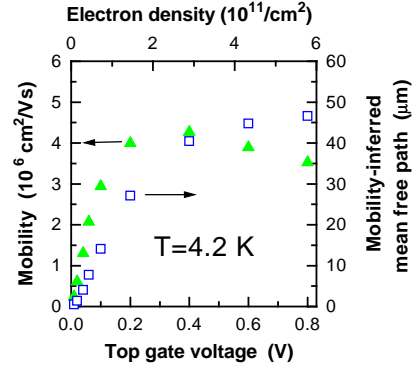


FIG. 2. Electron sheet density N , mobility μ (filled triangles), and mean free path (squares) calculated from N and μ , at $T = 4.2 \text{ K}$, for a UFET.

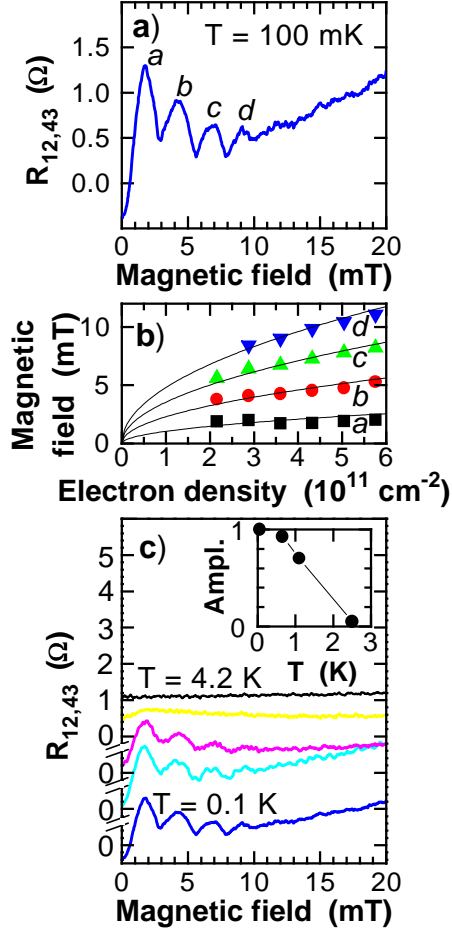


FIG. 3. (a) Magnetoresistance for $B \geq 0$. (b) Oscillation positions as a function of electron density. The solid curves are proportional to the square root of the electron density. (c) Oscillations at a range of temperatures: $T = 0.1, 0.65, 1.1, 2.5,$ and 4.2 K. Inset: graph of oscillation amplitude, defined as the change in resistance from the central minimum to the first B^+ peak, vs T .

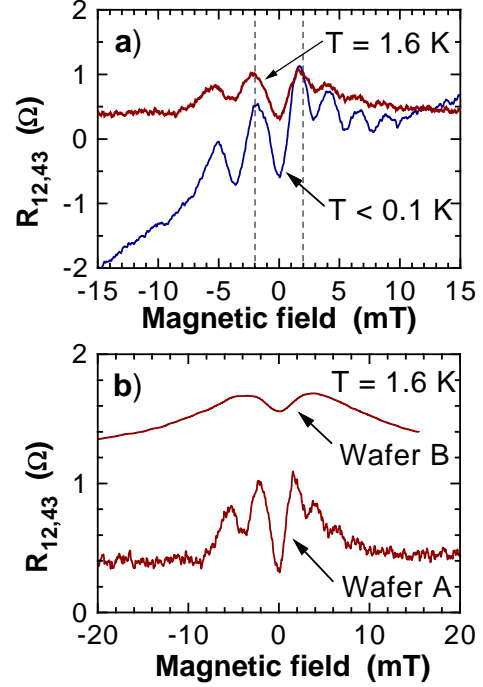


FIG. 4. (a) Magnetoresistance spanning $B = 0$, in the configuration of Fig. 1(c). Vertical, dotted lines indicate the expected positions of the first B^+ and B^- focusing peaks for a $100 \mu\text{m}$ square. (b) Comparison between two samples (from different wafers) at the same electron density.